Nanotechnology Perceptions
ISSN 1660-6795
www.nano-*ntp.com*

Fracture Analysis Of Low Pressure Shot Peened Dissimilar Weldments Of Super Austenite Stainless Steel And Ni-4Cu-3Mo Alloy By Laser Beam Welding

A. Thamarai Selvan[1,a], V. Vijaya Rajan[2,b], P. Arumugam[3,c], K. Paramasivam[4,d]

[1,4]Department of Mechanical Engineering, Saveetha Engineering College, Chennai, Tamilnadu, India, 602 105
[2]Department of Mechanical Engineering, Easwari Engineering College, Chennai, Tamilnadu, India, 600 089
[3]Department of Mechanical Engineering, Rajalakshmi Engineering College, Chennai, India 602 105
*[a]*thamsmechian@gmail.com, [b]vijayvr8@gmail.com, [c]arumugam.p@rajalakshmi.edu.in, [d]kparamasivam2004@gmail.com,*

In this research, fracture analysis was performed on low pressure shot peened (LPSP) dissimilar weldments of Super Austenite Stainless Steel (SASS) and Ni-4Cu-3Mo alloy by laser beam welding. The dissimilar joint of 2 mm thick sheets of SASS/Ni-4Cu-3Mo alloy was made on single side by laser beam welding with a heat input of 900W. The specimens were cut according to ASTM standards for tensile test. The tensile failures were observed on fusion zone of the weldment of dissimilar joint. The grain boundary growth was greatly affected by high heat input at fusion zone. The images obtained from Scanning Electron Microscope (SEM) confirmed about the absence of micro voids and pores. The LPSP on ferrite structures of weldment reduced the cracks and hole formation in materials. The LPSP process collapsed α-austenite structure and improved grain boundary growth. The transformation of α-ferrite structures into S-phase results in low fracture surface and higher elongation imparting better strength to the weldments.

Keywords: Super Austenite Stainless Steel, Low Pressure Shot Penning, Laser Welding, Dissimilar Joints, Fracture Analysis.

Introduction

The materials used in making components for defense, aerospace, automotive applications have to ensure the quality as failure may lead to greater mischievous results. In metallurgical failure analysis, the fracture surface and patterns are important to define the nature and cause of failure whether the failure happens due to sudden loads or fatigue loads. In a study on AL6XN Super Austenite stainless steel, the fatigue failure raised due to deformation on

dislocation slipping **[1].** The high stresses applied on the surface operated slip systems leading to rougher fracture surface. The failure of materials was greatly influenced by various forming or heat treatment and other manufacturing processes involved in making a product.

The tensile failure analysis performed on forged SASS UNS 20910 results with yield strengths ranged from 357 to 527 MPa **[2].** These larger variations in yield strength were due to grain boundary location and orientation. The crack growth rate played a vital role in determining the YS (1264-1620 MPa) at 4K in fatigue fracture test. A degradation mechanism was studied in cast austenite stainless steel (CASS) after thermal ageing and neutron irradiation **[3].** The two ferrite phases α-phase (Fe-rich) and α'-phase (Cr-rich) lead to nucleation and precipitate growth in ferrite – austenite boundary in CASS. The thermal ageing embrittlement in CASS was due to carbides and G-phase (Ni-rich). It was observed that hardness and chrome plating on AISIS D2 steel influence the crack initiation, its location, and the number of cracks developed **[4]** under 20,000 cycles of fatigue test. The cracks at lower surface were due to tension while on upper surface was due to compression. The crack initiation stopped at one stage because of low stress intensity factor. A decrease in plastic deformation was observed with the increase in hardness **[5].** The variation in hardness of two implant screws made of AISI 316L influenced the failure mechanism with severe plastic deformation. The microstructure study revealed that the failure occurred due to transformation of $\gamma 1 \rightarrow \varepsilon \rightarrow \alpha'$ phases.

The mechanical properties were greatly enhanced by shot peening process improving the surface properties like wear resistance and frictional resistance due to compressive residual stress induced on the surface of the materials **[6].** While investigating the fatigue performance of shot peened 304 ASS with intensities 0.1 mm A, 0.25 mm A and 0.4 mm A, no remarkable changes were observed in young's modulus, but the hardness was greatly improved **[7].** The shot peening process had induced more tensile stress concentration on the surface of 304 ASS under mechanical fatigue loading accelerating the release process at each cycle. Thus, the fatigue performance of the material was improved by shot peening process.

In our research, tensile and bending fracture analysis were performed on low pressure shot peened dissimilar weldments of Super Austenite Stainless Steel (Marine Steel) and Ni-4Cu-3Mo alloy after laser beam welded. Super austenite stainless steels are meant for high forming, corrosion resistance and finds more applications in high temperature environments. Marine austenitic steel welding was explored with rapid demands in marine engineering and industry. The stainlessness of the anticorrosive environment in coastal use and outside is an important requirement in many countries.

Experimental Methods

Materials Used. In the stainless-steel family, marine real steel [4] has been playing a very important role in the development of marine machinery and structure over the past few decades. The chemical compositions of the materials considered for this work are given in the **table 1**.

Table 1 Chemical Compositions of SASS and Ni-4Cu-3Mo alloy (in wt. %)

Alloy	Cr	Ni	Mo	Mn	N	C	Si	P	Cu	Fe
Super Austenite Stainless Steel	28.00	8.00	5.00	1.00	0.30	0.025	0.70	0.03	0.03	rest
Ni-4Cu-3Mo	21.00	35.00	3.00	2.00	-	0.06	1.00	0.035	0.05	rest

The **table 2** shows the mechanical properties of the dissimilar steel alloys used for laser beam welding.

Table 2 Mechanical properties of SASS and Ni-4Cu-3Mo alloy

Properties	SASS	Ni-4cu-3Mo alloy
Tensile Strength (MPa)	420	530
Ultimate Tensile Strength (MPa)	540	650
% Elongation	11.9	12.3

Laser Beam Welding. The mobility, physical properties and simplicity of various welding processes performed traditionally on dissimilar materials [1-3] of different thickness and shapes are well established. The material has undergone plastic decomposition due to the use of heat during the laser beam welding process [4-5]. This occurs with the temperature difference on the Asynchronous were created internal residual stresses. The laser beam welding parameters [6, 8, 9, 12] enhanced the quality of welding process with uniform distribution. This avoids surface damage and oxidation.

The dissimilar joint of 2 mm thick sheets of SASS/Ni-4Cu-3Mo alloy was made on single side by laser beam welding with a heat input of 900W. Since 2mm thick sheets were used for this investigation, laser beam welding was performed on single side as laser weld has high penetration. During laser welding of theses dissimilar metal joints, 8 mm focus distance and 250 mm/min welding speed were maintained. The welding parameters were considered by trial-and-error method.

Low Pressure Shot Peening. Generally shot peening on weldments of steel plates are very difficult [10]. Though, shot peening was performed on the laser beam weldments to improve the strength of the dissimilar joints [11]. The gas flow pressure was maintained at 15 kg/min at the FZ and HAZ of the dissimilar materials. Tiny balls of size 2 mm in diameter were used with this low pressure on weldment side during shot peening, At the same time deflection rate was minimized at the weldments.

Tensile and Bending Tests. ASTM E8/E8M-13 standard was used for making and testing all tensile samples and the tensile tests were conducted on Instron Universal Testing machine at 1 mm/min strain rate. The **figure 3 (a) & (b)** shows the tensile specimens made and tested with proposed dissimilar metals. ASTM E190/E192 standard was used to perform bending test considering three-point method at FZ and HAZ

Results and Discussion

The optical microscopic images of as LBW and LPSP dissimilar weldments at FZ are shown in the **figure 1.** At fusion zone of as welded dissimilar weldment, the microstructure shows more cracks and dimples on the surface **[figure 1 (a)].** These defects were greatly rectified after LPSP performed on the weldment of dissimilar joints at FZ. The surface had become smooth and micro holes and voids vanished **[figure 1 (b)].**

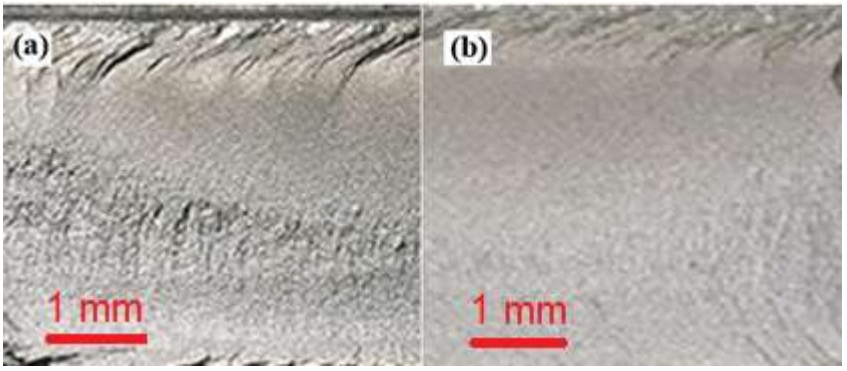

Fig. 1 Optical Microscopic images of fusion zone (a) LBW weldments (b) LBW+LPSP weldments

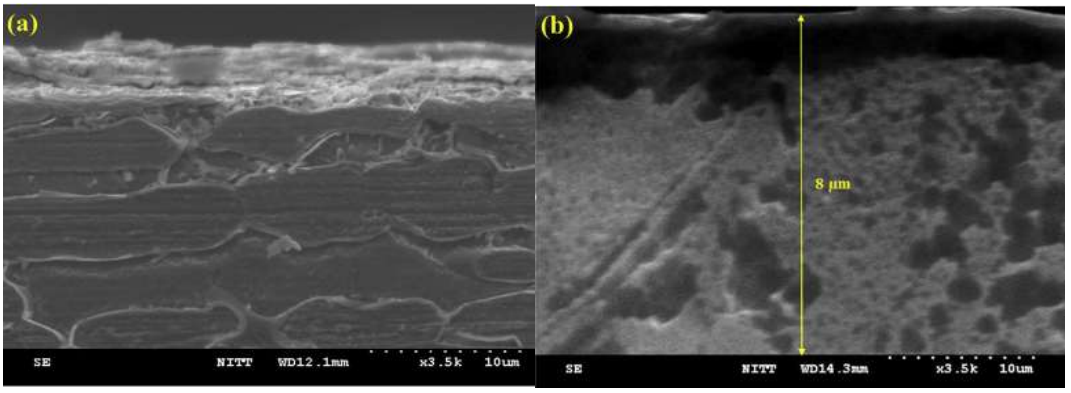

Fig. 2 SEM images of grain growth (a) LBW weldments (b) LPSP weldments

The grain growth of as LBW weldments at FZ after LPSP process are shown in **figure 2 (a) & (b).** The grain boundaries were greatly affected after LPSP.

Tensile tests were performed on the dissimilar weldments made after LBW and LPSP. As per ASTM E8/E8M-13 standard, overall length of the tensile specimens was maintained as 200±5 mm [**Figure 3 (a) & (b)**]. Loading was given gradually at 1 mm/min rate on three samples used for tensile tests with as welded and LPSP. The elongation ratio was found as 1.9, 2.25 and 2.18 % respectively for all the three specimens made by LBW. The elongation ratio had increased for base material compared to LBW and LPSP weldments. But the failures occurred only at FZ of each specimen.

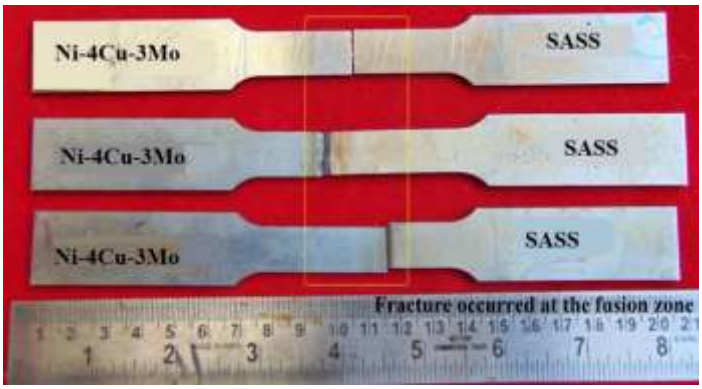

(a)

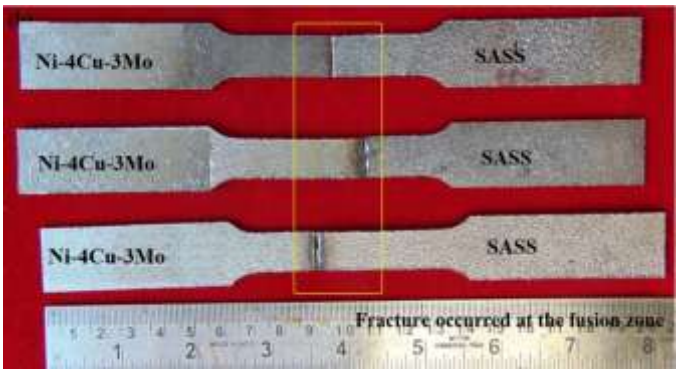

(b)

Fig. 3 Fractured tensile sample images of dissimilar weldments (a) after LBW (b) after LPSP

The surface morphology studies [**Figure 4 (a) & (b)**] revealed that α austenite phases were converted into α' martensite phases. The microstructures at FZ were homogeneous with ultimate strengths of 255, 270 and 440 MPa [F**igure 5 (a)**]. No cracks or holes were found at both FZ and HAZ.

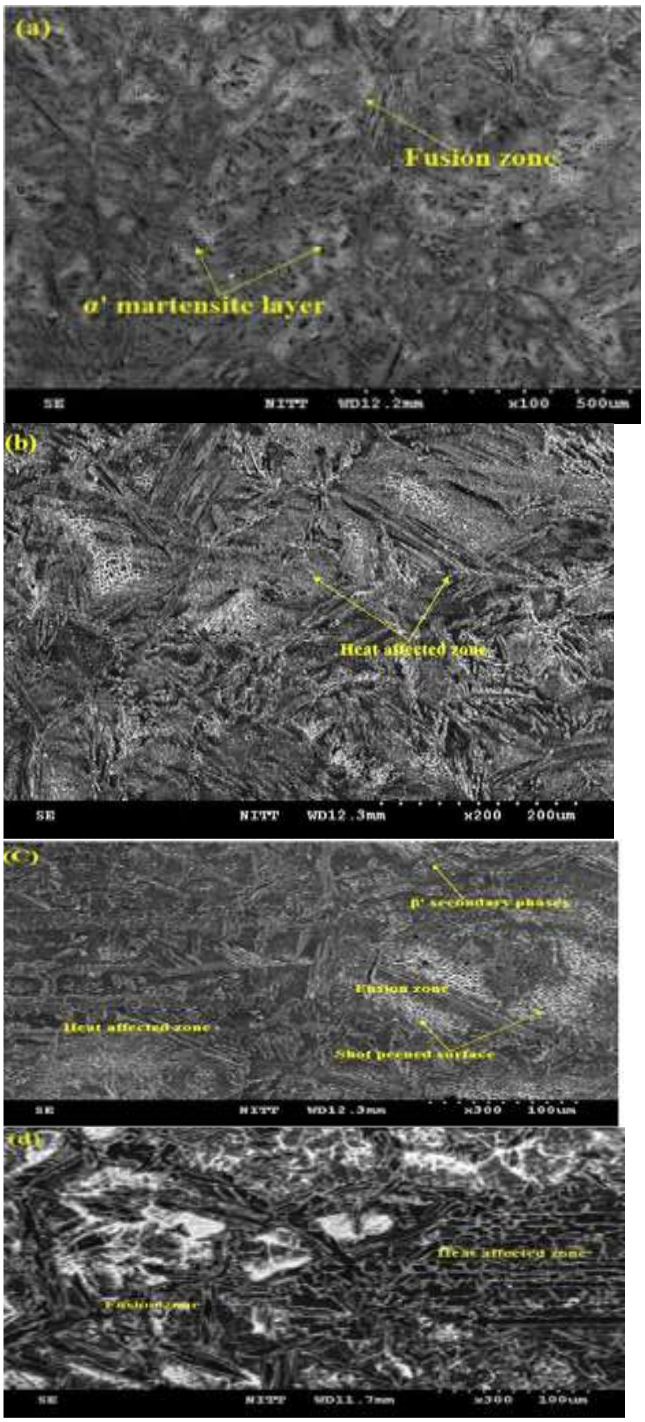
(a)
Fusion zone
α' martensite layer
SE NITT WD12.2mm x100 500um
(b)
Heat affected zone
SE NITT WD12.3mm x200 200um
(C)
β' secondary phases
Fusion zone
Heat affected zone
Shot peened surface
SE NITT WD12.3mm x300 100um
(d)
Heat affected zone
Fusion zone
SE NITT WD11.7mm x300 100um

Fig. 4 SEM images of (a) FZ of as welded (b) HAZ of SASS (c) LPSP weldments (d) HAZ of Ni-4Cu-3Mo alloy

The elongation ratio of LPSP weldments were found to be 6.99, 7.05 and 11.2% for all the three samples respectively. The **figure 3(b)** shows that failure of tensile specimens of LPSP weldments also had occurred at FZ. The O and B phases enhanced the hardness [8] of LPSP weldments from 258 HV to 275 HV with an average of 14% increase in elongation. This is due to compressive residual stress imparted on LPSP specimens [10-11]. **Figures 4 (a) & (b)** reveal that the grain boundary was affected to a larger extent. These SEM images clearly show the grain growth of LBW increased after LPSP. **Figure 4 (c) & (d)** shows that α ferrite structure was converted into twin boundaries and β' secondary phases throughout the FZ and HAZ of LPSP samples. The size of α' martensite structures was also increased greatly than coarse grains. Thus, the tensile tests on specimens of LBW and LPSP resulted with failures at FZ and not at HAZ. The results of tensile tests are shown in **figure 5 (a) & (b).**

LPSP process converted the ferrite boundaries were into twin boundaries and austenite structures that resulted in improved strength. In Ni-4Cu-3Mo alloy, the elements of Ni, C and Cr after high heat input converted the intermetallic structures into α' martensite and austenite structures. After LPSP, oxygen content was reduced at FZ and CrN and Cr2N phases were not seen [12]. The growth of grain boundaries was due to β and S Phases [13] which improved the mechanical properties and microstructures at FZ and HAZ.

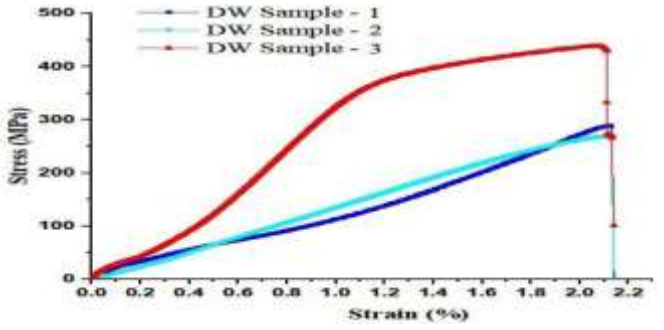

(a)

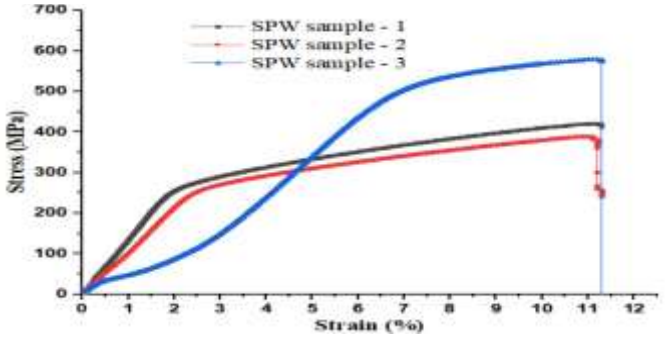

(b)

Fig. 5 Stress-Strain graphs on tensile analysis of dissimilar weldments (a) as LB welded (b) after LPSP

The stress strain curve in the **figure 5 (a)** shows that samples DW-1 and 2 behaved similarly at failures which trends gradually before their failures. The stress was minimum and more ductile with less strength before failure. The slope of the curve is lower which resulted with less stiffness. The sample DW-3 failed after reaching its maximum stress value and exhibited more brittleness and stronger. The slope of the curve is steeper which resulted with high stiffness. In the **figure 5 (b)**, sample SPW-1 shows more linear stress strain behaviour and SPW-2 failed little earlier than SPW-1. But sample SPW-3 failed at its peak stress than the other two samples. Due to strain hardening, it showed more resistance to deformation with 11.3 % strain and exhibited ductile fracture. The ductility of other two samples were 7 and 7.2% at their failures.

Conclusion

A fracture analysis was performed on the specimens made of LBW and LPSP processed dissimilar joints of SASS/ Ni-4Cu-3Mo alloy after tensile test. The failures of all tensile specimens of both as LBW and LPSP occurred at only the fusion zone. The elongation of LPSP processed joint showed an increase of 13% as an average compared to as LBW specimen. LPSP had improved the ultimate strength and microstructures at FZ with no hole or cracks on the weldments. The results showed the transformation of α austenite phases into α' martensite phases. There was more evidence on the grain boundary growth and transformation of ferrite structure into β' secondary phases and twin boundaries at FZ. The absence of CrN and Cr_2N intermetallic phases also improved the microstructure and mechanical strength of dissimilar joints of laser beam welded after LPSP.

References

[1] Karpagaraj A, Sankaranarayanasamy K, Some studies on mechanical properties and microstructural characterization of automated TIG welding of thin commercially pure titanium sheets, Materials Science and Engineering: A 640 (2015) 180-189

[2] Arivazhagan N, Singh S, Prakash S, Reddy GM, Investigation on AISI 304 austenitic stainless steel to AISI 4140 low alloy steel dissimilar joints by gas tungsten arc, electron beam and friction welding, Materials & Design 32 (2011) 3036-3050

[3] Enz, J, Kumar, M, Riekehr, S, Ventzke, V, Huber, N & Kashaev, N 2017, 'Mechanical properties of laser beam welded similar and dissimilar aluminum alloys', Journal of Manufacturing Processes, vol. 29, pp. 272-280.

[4] Nathan, SR, Balasubramanian, V, Malarvizhi, S & Rao, AG 2015, 'Effect of welding processes on mechanical and microstructural characteristics of high strength low alloy naval grade steel joints', Defence Technology, vol. 11, no. 3, pp. 308-317.

[5] Wu, W, Hu, S & Shen, J 2015, 'Microstructure, mechanical properties and corrosion behavior of laser welded dissimilar joints between ferritic stainless steel and carbon steel', Materials & Design, vol. 65, pp. 855-861.

[6] Jong-Guk Yuna, Chao-Qun Maa, Jiao-Jiao Yia, Xiao-Wu Li, Qualitative and quantitative characterizations of fracture surfaces of AL6XN super-austenitic stainless steel fatigued at different stress amplitudes, Progress in Natural Science: Materials International 22 (2012) 48–52

[7] D. M. McRae, R. P. Walsh, E. N. C. Dalder, S. Litherland, M. Trosen, D. J. Kuhlmann, Fatigue and fracture properties of a super-austenitic stainless steel at 295 K and 4 K, AIP Conference Proceedings 1574 (2014) 59-66

[8] Furqan Mukhtar, Faisal Qayyum, Zeeshan Anjum, Masood Shah, Effect of chrome plating and varying hardness on the fretting fatigue life of AISI D2 components, Wear 418–419 (2019) 215–225

[9] Alfonso Monzamodeth Román-Sedano, Bernardo Campillo, Fermín Castillo, Osvaldo Flores, Failure Analysis of Austenitic Stainless Steel Implant Screws and Prospection of Chemical
Composition Using Artificial Intelligence, World Journal of Engineering and Technology 10 (2022) 98-118

[10] R. Gopi, I. Saravanan, A. Devaraju, Ganesh babu Loganathan, Investigation of shot peening process on stainless steel and its effects for tribological applications, Materials Today: Proceedings 22 (2019) 1-5

[11] Shun Yang, Wu Zeng, Jishen Yang, Characterization of shot peening properties and modelling on the fatigue, performance of 304 austenitic stainless steel, International Journal of Fatigue 137 (2020) 105621

[12] Xu QIN, Xinqian ZHAO, Zhaoyang JIN, Qinghang WANG, Yield Stress and Elongation Prediction and Process Parameter Optimization of Two C-Mn Steels Based on XG Boost and Non-dominated Sorting Genetic Algorithm-II, Materials Science (Medžiagotyra) 30 (2024) 327-333

[13] Sarra KHELIFI, Abdelhak AYAD, Ahcene BOUMAIZA, Nadjet ROUAG, Francis WAGNER, Vincent JI, Correlations Between XRD Peak Broadening and Elastic and Plastic Deformation for Mild Steel Sheets Under Tensile Loading, Materials Science (Medžiagotyra) 30 (2024)